Local secondary-electron emission spectra of graphite and gold surfaces obtained using the

Scanning Probe Energy Loss Spectrometer (SPELS)

Local secondary-electron emission spectra of graphite and gold surfaces obtained using the Scanning Probe Energy Loss Spectrometer (SPELS)

J J Lawton, A Pulisciano and R E Palmer

Nanoscale Physics Research Laboratory, School of Physics and Astronomy,
University of Birmingham, Birmingham B15 2TT, UK

E-mail: R.E.Palmer@bham.ac.uk

Abstract
Secondary-electron emission (SEE) spectra have been obtained with the Scanning Probe Energy
Loss Spectrometer at a tip–sample distance of only 50 nm. Such short working distances are
required for the best theoretical spatial resolution ($<$10 nm). The SEE spectra of graphite,
obtained as a function of tip bias voltage, are shown to correspond to unoccupied states in the
electronic band structure. The SEE spectra of thin gold films demonstrate the capability of
identifying (carbonaceous) surface contamination with this technique.

1. Introduction

The increasing level of control over the properties of materials on the nanometre scale is driving the creation of new types of instruments for nanometrology. One such instrument is the Scanning Probe Energy Loss Spectrometer (SPELS) [1–10]. Recently Yin *et al* [11] exploited the SPELS instrument to obtain characteristic SEE peaks from graphite, i.e., in addition to the energy loss features associated with the π and $(\pi + \sigma)$ surface plasmons [1]. In our work, the tip–sample distance employed was in the range 50–3000 nm. However, theoretical treatment of the ultimate spatial resolution possible with SPELS [3] makes the use of smaller tip–sample distances ($<$50 nm) desirable. In this paper we report (a) the successful acquisition of both SPELS and SPELS-SEE spectra at tip distances of 50 nm and (b) the sensitivity of the SEE spectra to surface contamination.

2. Experimental details

The SPELS instrument employed in this work [11] combines an ultrahigh vacuum scanning tunnelling microscope (UHV-STM) manufactured by Omicron (STM-1), modified by ourselves to shield the high electric fields generated by the field emission bias voltage, and a hemispherical electron energy analyser (VG100AX), with entrance slit width 4 mm. The nose of the analyser is located approximately 4 cm above the STM tunnel junction, parallel to the sample surface. STM tips were electrochemically etched in a 2.0 M sodium hydroxide (Aldrich) solution using straight cut pieces of temper annealed tungsten wire (Advent Research Materials). The tips were subsequently cleaned *in situ* via electron bombardment heating to remove any residual tungsten oxide left behind from the etching process. This process acts to improve the field emission performance of the tips. Graphite (highly oriented pyrolytic graphite, HOPG) samples were cleaved in air and immediately loaded into the UHV system via a fast load lock. Gold films were produced by evaporating gold (99.99%) onto freshly cleaved HOPG in an evaporator at a base pressure of $\sim 1 \times 10^{-6}$ mbar, with the sample heated to 350 °C during the evaporation. Film thickness was measured with a surface profiler (Veeco Dektak) and found to be in excess of 100 nm; the samples were thus exposed to air prior to loading into the UHV system. One sample was transferred directly to the STM for analysis without any further processing (hereafter referred to as the 'native' sample). A second sample was subjected to two cycles of annealing/argon ion sputtering (annealing at 500 °C for 1 h and sputtering at 0.5 keV for 15 min); this sample was left in the UHV chamber for two days at a pressure of $\sim 1 \times 10^{-9}$ mbar before measurements were
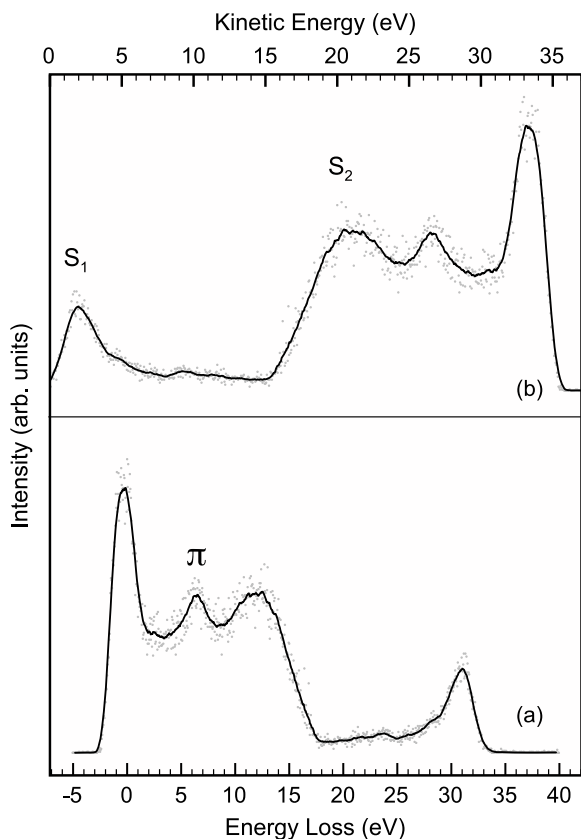
Figure 1. SPELS spectra of graphite at a tip–sample working distance of 50 nm and a tip bias voltage of −37.5 V. (a) Electron energy loss spectrum, with the π-plasmon energy loss peak labelled. (b) The same data presented in terms of kinetic energy relative to the vacuum level (graphite work function 4.5 eV); two secondary-electron peaks, S_1 and S_2, are highlighted.

taken (and is referred to as the 'cleaned' sample). Gold films were confirmed to be polycrystalline through the observation of domain boundaries (with domain sizes of a few hundred nm) using the SPELS instrument in STM mode.

3. Results

3.1. Secondary-electron emission from graphite

Figure 1(a) shows SPELS data presented from graphite and is the first demonstration of SPELS spectra obtained at a tip–sample working distance as small as 50 nm and bias voltage as small as −37.5 V. Such working distance and bias voltage suggest [3] that a spatial resolution of less than 5 nm is possible (in future measurements). Yin *et al* [11] investigated SPELS-SEE from the same graphite surface at a much larger working distance of ~1000 nm. Figure 1(a) exhibits a single energy loss feature, the well known π-plasmon of graphite, as well as two fixed kinetic energy peaks associated with secondary electrons (see figure 1(b) where the data set is replotted; graphite work function 4.5 eV). These two features were confirmed to be fixed kinetic energy peaks by changing the tip bias (and therefore the incident electron energy) and observing whether the peaks shift relative to the elastic peak in the energy loss spectrum.
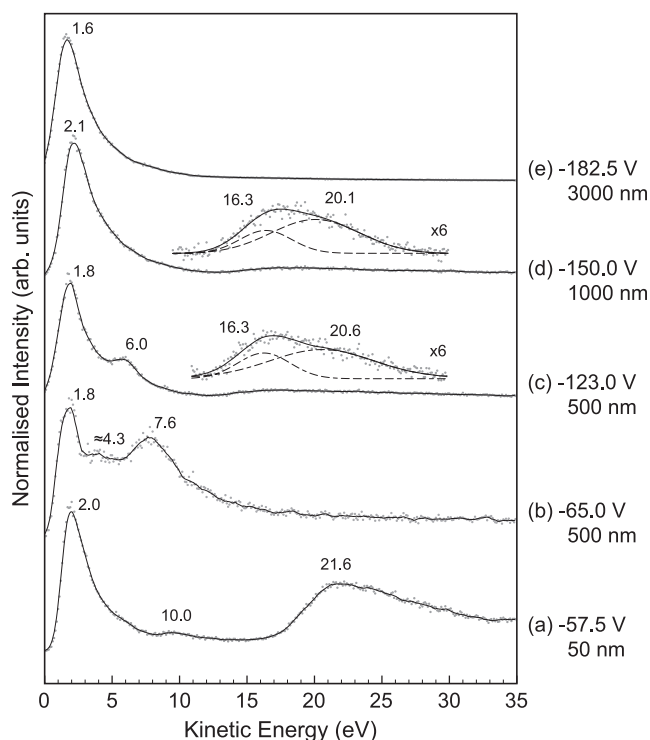

Figure 2. Secondary-electron emission spectra in SPELS of graphite taken at different tip bias voltages and tip–sample working distances. (a) −57.5 V, 50 nm; (b) −65.0 V, 500 nm; (c) −123.0 V, 500 nm; (d) −150.0 V, 1000 nm; (e) −182.5 V, 3000 nm. The kinetic energy is given relative to the vacuum level.

The secondary-electron emission spectra of surfaces generally exhibit a characteristic peak in the low kinetic energy region (~2 eV). This peak is known as the 'cascade' peak, since it results from a cascade of inelastic scattering events [12–14] suffered by the incident electrons. The energy of this peak is generally independent of the incident electron energy or direction with respect to the surface. In addition to the cascade peak, extra peaks are also seen at specific, higher kinetic energies. Early work on graphite by Willis *et al* showed [15, 16] that such peaks can be correlated with transitions of electrons into specific unoccupied states in the electronic band structure before they leave the surface (the correlation is not confined to graphite [17–19]). Thus in figure 1(b) the secondary-electron feature, S_1, which occurs at 2.0 eV is the cascade peak, but we assign the S_2 feature at ~21.0 eV to unoccupied states in the graphite band structure (see below).

Figure 2 shows a series of SPELS-SEE spectra from graphite taken at different tip bias voltages and tip–sample working distances. The peak positions labelled were determined by fitting single or multiple peaks after a polynomial background subtraction. Figure 2(a) shows an asymmetric peak at about 22 eV which was fitted using two Gaussians (dashed lines). Figures 2(c) and (d) both show peaks at about 18 eV and both were fitted using two Gaussian functions (dashed lines). The data show that the intensities of the secondary-electron emission features in SPELS are strongly dependent upon the tip bias and working distance,

Table 1. Secondary-electron emission of graphite as observed in SPELS with proposed band assignments. Comparison with other experimental and theoretical work is made. All energies are in eV and are referenced relative to the vacuum level. SEE = secondary-electron emission, SPELS-SEE = scanning probe energy loss spectroscopy and secondary-electron emission, IP = inverse photoemission spectroscopy, TCS = target current spectroscopy, NA = not available.

Band assignment	Experimental (eV, this work)	Previous experimental (eV)	Theory (eV)
$\sigma(\Gamma_5^+, \Gamma_6^-)$[a]	4.3	5.0 (IP)[b], 5.2 (IP)[c], 4.5 (IP)[d]	4.5[e]
$\pi(\Gamma_3^+)$[a,f]	6.0	6.0 (SPELS-SEE)[g], 5.0 (IP)[b], 5.2 (IP)[c]	5.8[e]
$\sigma(\Gamma_1^+, \Gamma_4^-)$[h,f]/$\pi(\Gamma_3^+)$[f,i]	7.6	7.0 (SEE)[i], 7.5 (IP)[b]	8.4[e], 7.0[j]
π[h]	10.0	11.5 (SPELS-SEE)[g], 12.5 (IP)[c]	NA
$\sigma(\Gamma_4^-)$[h,f]	16.3	17.5 (SPELS-SEE)[g], 15.0 (IP and TCS)[c], 16.0 (IP)[d], 16.5 (SEE)[i]	17.0[j]
$\sigma(\Gamma_1^+)$[f]/$\sigma(\Gamma_4^-)$[h]	20.1 20.6 21.6	19.5 (TCS)[c], 20.0 (IP)[c], 19.3 (SEE)[i]	20.6[j]/21.5[j]

[a] Band assignment from [21].
[b] Ref. [26]; values taken at $k_{\parallel} = 0$.
[c] Ref. [22]; values taken at $k_{\parallel} = 0$.
[d] Ref. [24]; values taken at $k_{\parallel} = 0$.
[e] Ref. [21]; values taken at $k_{\parallel} = 0$.
[f] Band assignment from [23].
[g] Ref. [11]; measured at 7° from the sample plane.
[h] Band assignment from [22].
[i] Ref. [25]; values taken at $k_{\parallel} = 0$.
[j] Ref. [23]; values taken at $k_{\parallel} = 0$.

which together regulate the electric field in the region between the tip and sample. In turn, this electric field affects the trajectories of electrons emerging from the surface and thus which electrons are ultimately detected by the analyser. As previously reported [11], the SPELS-SEE peak positions (but not intensities) for graphite agree well with data collected by a conventional SEE spectrometer [20] with the electrons coming principally from the vicinity of the zone centre (Γ) in the band structure.

Table 1 displays the proposed band assignments for the peaks in figure 2. The peak in each spectrum at ∼2 eV is not included since it is assigned to the cascade peak. All other peaks are assigned to particular unoccupied states. The assignments were made by considering mainly the theoretical calculations of Holzwarth *et al* [21] and Tatar and Rabii [23] as well as the experimental work (conventional SEE) of Caputi *et al* [25]. The calculations of Holzwarth *et al* only extend up to 7.5 eV relative to the vacuum level, so the calculations of Tatar and Rabii were used for making assignments for the higher energy states, extending up to 24.5 eV relative to the vacuum level. The work of Holzwarth *et al* was chosen in preference to that of Tatar and Rabii for making the low energy band assignments since their work is in better agreement with experimental measurements [22, 24, 26]. The SPELS-SEE measurements of this work are also compared with previous experimental data, including inverse photoemission spectroscopy [22, 24, 26], target current spectroscopy [22], conventional SEE spectroscopy [25] and previous SPELS-SEE [11]. Most of the assignments in table 1 correspond to relatively flat bands near the zone centre (Γ).

3.2. Secondary-electron emission of gold

In figure 3 the SPELS-SEE spectra from both (a) the cleaned and (b) the native gold film samples are shown. Figure 3(a) for the cleaned gold film shows the typical single-cascade peak observed for polycrystalline metal surfaces [17, 18, 27]. Figure 3(b) for the native (contaminated) gold film, however, shows a second peak (at ∼5.7 eV) in addition to the cascade peak. It is proposed that this extra peak is related to some kind of surface contamination. In order to explain the presence of this feature, one of the spectra for graphite (from figure 2(c)) is reproduced for comparison as figure 3(c). All the spectra in figure 3 are normalized to their cascade peaks. The graphite spectrum, figure 3(c), shows a peak at similar kinetic energy (∼6 eV) to the native gold sample, figure 3(b), but with a different intensity relative to the cascade peak. A possible explanation of the contaminant peak for gold is thus that this feature corresponds to carbonaceous material. Hoffman *et al* [28] have reported various peaks additional to the cascade maxima in conventional SEE spectra of a number of carbonaceous materials. Carbonaceous surface contamination is reasonable for a sample transferred from the atmosphere to a UHV chamber via a load lock and without any cleaning.

4. Summary

In summary, the acquisition of SPELS and SPELS-SEE spectra at tip–sample distances as small as 50 nm has been demonstrated (for graphite) and the sensitivity of such SPELS-SEE spectra to surface contamination (on gold) has also been shown. Band assignments for the SPELS-SEE features of graphite have been proposed, indicating that the electrons observed come predominantly from flat bands near the zone
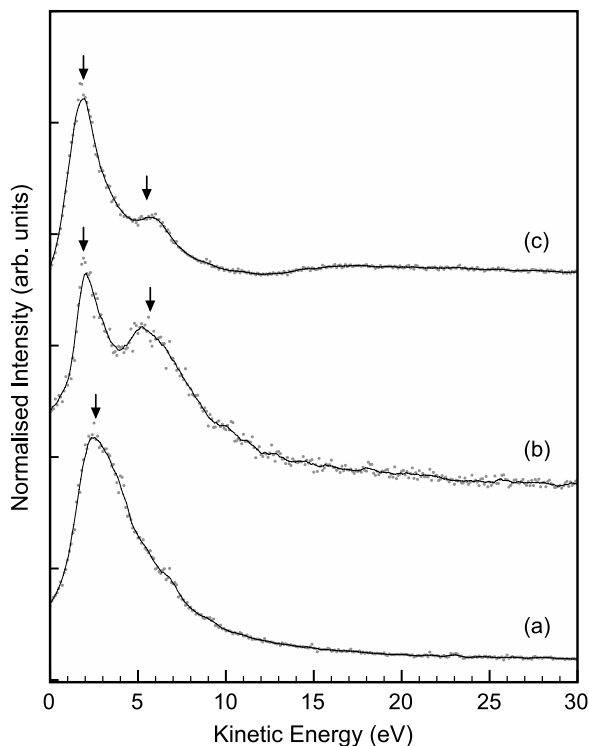
Figure 3. SPELS spectra showing the secondary-electron emission features of (a) gold film after cleaning, tip bias voltage −200 V, working distance 480 nm; (b) native gold film, tip bias voltage −260 V, working distance 480 nm; (c) graphite, reproduced for comparison from figure 2(c), tip bias voltage −123 V, working distance 500 nm. The kinetic energy is given relative to the vacuum level. The spectra are normalized to the cascade secondary-electron emission peak at ∼2 eV.

centre. The intensities of the SEE peaks appear to depend on the electric field between tip and surface, as determined by the tip shape, applied voltage and working distance. Future measurements with screened tips should therefore be intriguing.

Acknowledgments

References

[1] Eves B J, Festy F, Svensson K and Palmer R E 2000 *Appl. Phys. Lett.* **77** 4223–5
[2] Festy F, Svensson K, Laitenberger P and Palmer R E 2001 *J. Phys. D: Appl. Phys.* **34** 1849–52
[3] Palmer R E, Eves B J, Festy F and Svensson K 2002 *Surf. Sci.* **502** 224–31
[4] Palmer R E 2002 *Surf. Interface Anal.* **34** 3–9
[5] Festy F and Palmer R E 2004 *Appl. Phys. Lett.* **85** 5034–6
[6] Miyatake Y, Nagamura T, Hattori K, Kanemitsu Y and Daimon H 2003 *Japan. J. Appl. Phys.* **42** 4848–51
[7] Hirade M, Arai T and Tomitori M 2006 *Japan. J. Appl. Phys.* **45** 2278–82
[8] Mizuno S, Rahman F and Iwanaga M 2006 *Japan. J. Appl. Phys.* **45** L178–9
[9] Hammadi Z and Morin R 2006 *Ultramicroscopy* **106** 480–5
[10] Zhou X, Xu C, Wei Z, Liu W, Li J, Chen X, Williams J F and Xu K 2008 *J. Electron Spectrosc. Relat. Phenom.* **165** 15–9
[11] Yin J, Pulisciano A and Palmer R E 2006 *Small* **2** 744–6
[12] Wolff P A 1954 *Phys. Rev.* **95** 56–66
[13] Modinos A 1984 *Field, Thermionic, and Secondary Electron Emission Spectroscopy* (New York: Plenum)
[14] Komolov S A 1992 *Total Current Spectroscopy of Surfaces* (Philadelphia, PA: Gordon and Breach) chapter 3
[15] Willis R F, Feuerbacher B and Fitton B 1971 *Phys. Lett.* A **34** 231–3
[16] Willis R F, Feuerbacher B and Fitton B 1971 *Phys. Rev.* B **4** 2441–52
[17] Seah M P 1969 *Surf. Sci.* **17** 132–60
[18] Panchenko O F and Panchenko L K 2007 *Vacuum* **81** 766–70
[19] Panchenko O F 2002 *J. Electron Spectrosc. Relat. Phenom.* **127** 11–6
[20] Papagno L, Caputi L S, De Crescenzi M and Rosei R 1982 *Phys. Rev.* B **26** 2320–2
[21] Holzwarth N A W, Louie S G and Rabii S 1982 *Phys. Rev.* B **26** 5382–90
[22] Schäfer I, Schlüter M and Skibowski M 1987 *Phys. Rev.* B **35** 7663–70
[23] Tatar R C and Rabii S 1982 *Phys. Rev.* B **25** 4126–41
[24] Ohsawa H, Takahashi T, Kinoshita T, Enta Y, Ishii H and Sagawa T 1987 *Solid State Commun.* **61** 347–50
[25] Caputi L S, Chiarello G, Santaniello A, Colavita E and Papagno L 1986 *Phys. Rev.* B **34** 6080–4
[26] Collins I R, Andrews P T and Law A R 1988 *Phys. Rev.* B **38** 13348–54
[27] Koshikawa T and Shimizu R 1973 *J. Phys. D: Appl. Phys.* **6** 1369–80
[28] Hoffman A, Prawer S and Kalish R 1992 *Phys. Rev.* B **45** 12736–5